

Catalytic oxidation of organic sulfides by H₂O₂ in the presence of titanosilicate zeolites

Marcelina Radko^a, Małgorzata Rutkowska^{a,**}, Andrzej Kowalczyk^a, Paweł Mikrut^a,
Aneta Świąć^a, Urbano Díaz^b, Antonio E. Palomares^b, Wojciech Macyk^a, Lucjan Chmielarz^{a,*}

^a Jagiellonian University, Faculty of Chemistry, Gronostajowa 2, 30-387, Kraków, Poland

^b Instituto de Tecnología Química, Universitat Politècnica de València – Consejo Superior de Investigaciones Científicas, Avd. de los Naranjos s/n, 46022, Valencia, Spain

ARTICLE INFO

Keywords:

Ti-ITQ-6
Ti-FER
Diphenyl sulfide
Dimethyl sulfide
Oxidation
H₂O₂
Catalysis

ABSTRACT

Titanosilicate ferrierite zeolite (FER) and its delaminated form (ITQ-6), with various Si/Ti molar ratios, were synthesized and tested as catalysts for diphenyl sulfide (Ph₂S) and dimethyl sulfide (DMS) oxidation with H₂O₂. The zeolites were characterized with respect to their chemical composition (ICP-OES), structure (XRD, UV–vis DRS) and texture (low-temperature N₂ adsorption-desorption). Titanium in the FER and ITQ-6 samples was present mainly in the zeolite framework with a significant contribution of titanium in the extraframework positions. Titanosilicate zeolites of FER and ITQ-6 series were found to be active catalysts of diphenyl and dimethyl sulfides oxidation by H₂O₂ to sulfoxides (Ph₂SO/DMSO) and sulfones (Ph₂SO₂/DMSO₂). The efficiency of these reactions depends on the porous structure of the zeolite catalysts – conversion of larger molecules of diphenyl sulfide was significantly higher in the presence of delaminated zeolite Ti-ITQ-6 due to the possibility of the interlayer mesopores penetration by reactants. On the other side diphenyl sulfide molecules are too large to be accommodated into micropores of FER zeolite. The efficiency of dimethyl sulfide conversion, due to relatively small size of this molecule, was similar in the presence of Ti-FER and Ti-ITQ-6 zeolites. For all catalysts, the organic sulfide conversion was significantly intensified under UV irradiation. It was suggested that Ti cations in the zeolite framework, as well as in the extraframework, species play a role of the single site photocatalysts active in the formation of hydroxyl radicals, which are known to be effective oxidants of the organic sulfides.

1. Introduction

Zeolites have been known as very important materials for catalysis since their successful application in petrochemistry in the 60's of 20th century [1]. Since that time many new zeolite topologies and their applications in industry have been developed. One of the most interesting synthetic zeolite is ferrierite (FER), based on the 5-membered rings (MR) with two types of perpendicularly intersecting channels (delimited by 8 and 10 MR) [2]. Precursors of ferrierite, PREFER, are characterized by the layered structure, in which the zeolite sheets are separated by surfactant molecules. During their calcination organic surfactants are removed from PREFER resulting in the condensation of silanol groups from the pinnately placed layers with the formation of 3D microporous structure of FER [2]. The specific layered structure of PREFER gives also an opportunity to obtain delaminated zeolitic materials, characterized by the hierarchical microporous and mesoporous structure [3]. Such

delaminated zeolitic materials, called ITQ-6, and also microporous FER are very interesting as catalysts or catalytic supports for various chemical process [4]. Their applicability is related not only to the porous structure but also to the presence of acid sites, as well as ion-exchange properties and therefore possibility of uniform deposition of catalytically active metal ions [4–7]. Moreover, a very important advantage represented by ITQ-6 is its delaminated structure consisting of larger pores located between chaotically arranged zeolite layers and micropores inside zeolite layers. Such hierarchical porous structure was reported to be effective in the conversion of bulkier molecules due to reduced internal diffusion restrictions of reactants. Examples of this effect are comparative studies of Ti-FER and Ti-ITQ-6 based catalysts for epoxidation of 1-hexene with H₂O₂ [5,8] or styrene epoxidation with tertbutyl hydroperoxide [7]. Titanium substituted into the zeolite framework results in the modification of its acidic character. Titanosilicate zeolites have been reported to be more effective in binding and

* Corresponding author.

** Corresponding author.

E-mail address: chmielar@chemia.uj.edu.pl (L. Chmielarz).

<https://doi.org/10.1016/j.micromeso.2020.110219>

Received 31 December 2019; Received in revised form 20 March 2020; Accepted 26 March 2020

Available online 19 April 2020

1387-1811/© 2020 The Authors. Published by Elsevier Inc. This is an open access article under the CC BY license (<http://creativecommons.org/licenses/by/4.0/>).

activation of some organic molecules and therefore have been known to be efficient catalysts for various oxidation processes [9]. An example is application of Ti-zeolites – TS-1, TS-2, Ti-beta – as effective catalysts for the selective oxidation of diphenyl, methyl phenyl and dipropyl sulfides [10]. One of the main problems of bulky organic sulfides oxidation is related to the internal diffusion limitations of bulky reactants inside pores. To overcome this problem the zeolitic catalysts with the combined micro-mesoporous structure can be used [9–11]. Internal diffusion of bulky molecules in mesopores is much faster than in micropores and therefore the overall reaction rate in the case of the catalysts with the hierarchical micro-mesoporous structure should be much faster comparing to microporous catalysts. Many organic sulfides, e.g. dimethyl sulfides, diphenyl sulfides and products of their oxidation, organic sulfoxide and sulfones, are important chemicals for various applications, including pharmacy and medicine. They are used in production of various pharmaceuticals, such as vasodilators, psychotropics, antiulcer and antihypertensive medications, as well as antibacterial and antifungal agents. Organic sulfoxide and sulfones can be produced by selective oxidation of suitable organic sulfides. Among various oxidizing agents hydrogen peroxide, H_2O_2 , which is nontoxic, clean and produces only water as by-product, seems to be the most promising one [12,13]. Our previous studies have shown very promising results of diphenyl sulfides oxidation to diphenyl sulfoxide and sulfone by H_2O_2 in the presence of TiO_2 -based catalysts [14]. These studies were extended for titanosilicate zeolites, Ti-FER and Ti-ITQ-6, used as catalysts in the process of dimethyl and diphenyl sulfides oxidation using hydrogen peroxide as an oxidant with and without UV irradiation.

2. Experimental

2.1. Synthesis of catalysts

Two series of the zeolitic samples, Ti-FER and Ti-ITQ-6, with different Si/Ti molar ratios were prepared based on the recipe reported earlier [3]. Ti-PREFER materials were synthesized using fumed silica (Aerosil 200, silicon source), titanium (IV) ethoxide (TEOTi, titanium source), 4-amino-2,2,6,6-tetramethylpiperidine (R, structure directing agent), NH_4F , HF and distilled water in the following molar ratios – 1 SiO_2 : x TEOTi: 1 R: 1.5 NH_4F : 0.5 HF: $10\text{H}_2\text{O}$, where $x = 0.08, 0.04, 0.02$ and 0.01 for the intended Si/Ti molar ratios equal to 12.5, 25, 50 and 100, respectively. The obtained gels were continuously stirred in autoclaves at $135\text{ }^\circ\text{C}$ for 10 days. The resulting solid products were filtered, washed with distilled water and dried at $60\text{ }^\circ\text{C}$. The synthesis resulted in four Ti-PREFER samples with the attended Si/Ti molar ratios of 12.5, 25, 50 and 100, denoted as Ti-PREFER-12.5, Ti-PREFER-25, Ti-PREFER-50 and Ti-PREFER-100, respectively.

Each of the obtained Ti-PREFER samples was divided into two portions. The first one was calcined at $650\text{ }^\circ\text{C}$ for 10 h resulting in the condensation of the ferrierite layers with the formation of three dimensional microporous ferrierite zeolites with the intended Si/Ti molar ratios of 12.5, 25, 50 and 100, denoted as Ti-FER-12.5, Ti-FER-25, Ti-FER-50 and Ti-FER-100, respectively. The second part of the Ti-PREFER samples was dispersed in a solution consisting 40 g of H_2O , 200 g of cetyltrimethylammonium bromide (CTMABr, 25 wt%, 50% exchanged Br/OH) and 60 g of tetrapropylammonium bromide (TPABr, 40 wt%, 30% exchanged Br/OH) and refluxed at $80\text{ }^\circ\text{C}$ for 16 h. Then, the slurries were sonicated in an ultrasound bath (50 W, 40 kHz) for 1 h to disperse the swollen ferrierite sheets. In the next step pH of slurries was decreased to about 3.0 with the use of concentrated HCl and then the solid samples were recovered by centrifugation and washed with distilled water. After drying at $60\text{ }^\circ\text{C}$ and calcination at $650\text{ }^\circ\text{C}$ for 10 h, a series of the Ti-ITQ-6 samples with the intended Si/Ti molar ratios of 12.5, 25, 50 and 100, denoted as Ti-ITQ-6-12.5, Ti-ITQ-6-25, Ti-ITQ-6-50 and Ti-ITQ-6-100, respectively, was obtained.

2.2. Characterization of the zeolite samples

The obtained zeolite materials were characterized with respect to their chemical composition, structure and texture. The chemical composition of the samples was determined by ICP-OES method using an iCAP 7400 instrument (Thermo Science). The solid samples were dissolved in a mixture of hydrofluoric, hydrochloric and nitric acid solutions assisted by microwave radiation using Ethos Easy system (Milestone). X-ray diffractograms of the zeolite samples were obtained using Bruker D2 diffractometer. The measurements were performed with $\text{Cu-K}\alpha$ radiation in the 2 Theta range of $2\text{--}45^\circ$ with a step of 0.02° and a counting time of 1 s per step. Textural properties of the samples were determined by N_2 adsorption-desorption measurements at $-196\text{ }^\circ\text{C}$ using a 3 Flex (Micrometrics) automated gas adsorption system. Prior to measurements, the samples were outgassed under vacuum at $350\text{ }^\circ\text{C}$ for 24 h. The specific surface area value was determined using BET equation. Distributions of micropore sizes were determined using the Horvath-Kawazoe model, while for the mesopore range according to BJH model. The total pore volume was determined by means of the total amount of adsorbed nitrogen at $p/p_0 = 0.98$. Micropore volume was determined using the t-plot method. The UV–vis diffuse reflectance spectra of the samples were measured at room temperature using an Evolution 600 (Thermo Science) spectrophotometer. The spectra were recorded in the range of $190\text{--}900\text{ nm}$ with a resolution of 4 nm.

2.3. Catalytic tests

The zeolitic samples of Ti-FER and Ti-ITQ-6 series were tested as catalysts for oxidation of diphenyl (Ph_2S) and dimethyl (DMS) sulfides to sulfoxides ($\text{Ph}_2\text{SO}/\text{DMSO}$) and sulfones ($\text{Ph}_2\text{SO}_2/\text{DMSO}_2$) in the presence of hydrogen peroxide (H_2O_2) as an oxidant. The reaction was performed in a 100 cm^{-3} round-bottom flask equipped with stirrer, dropping funnel and thermometer. The reaction mixture consisted of 0.4 mmol of diphenyl sulfide (or dimethyl sulfide, DMS), 20 cm^{-3} of acetonitrile used as a solvent, 0.1 mmol of bromobenzene used as an internal standard and 25 mg of the catalyst. The obtained mixture was stirred (1000 rpm) at $25\text{ }^\circ\text{C}$ for 10 min and then 2 mmol of hydrogen peroxide (30% solution of H_2O_2) was added. The catalytic reaction was performed in the dark in order to avoid photocatalytic conversion of Ph_2S (conditions marked here as “DARK”). Moreover, the reaction was also performed under UV irradiation (marked as “LIGHT”). In this case a 150 W xenon short arc lamp was used as a UV light source (11.65 mW cm^{-2}). To avoid excitation of Ph_2S and its direct photooxidation a 320 nm cut off filter was applied, as well as a NIR and IR filter (10 cm optical path, 0.1 mol dm^{-3} solution of CuSO_4). The reaction progress was monitored by analysis of the reaction mixture by HPLC method. The mixture of acetonitrile/water with the volume ratio of 80:20 was used as the eluent. The samples of the reaction mixture were taken in regular intervals – every 10 min within the first hour and every 30 min afterwards, filtered through the $0.22\text{ }\mu\text{m}$ Nylon membrane filter and analysed at a Flexar chromatograph (PerkinElmer) equipped with the analytical C18 column ($150\text{ mm} \times 4.6\text{ mm i.d.}$, $5\text{ }\mu\text{m}$ pore size). The column was maintained at $25\text{ }^\circ\text{C}$ throughout analysis and the UV detector was set at 254 nm for oxidation of Ph_2S or 210 nm for oxidation of DMS. Catalytic and photocatalytic tests were conducted with the over-stoichiometric excess of H_2O_2 ($\text{H}_2\text{O}_2/\text{sulphide}$ molar ratio of 5). In such conditions the reaction rate is not limited by the actual content of H_2O_2 in the reaction mixture. The examples of the results of the photocatalytic tests conducted with different $\text{H}_2\text{O}_2/\text{Ph}_2\text{S}$ molar ratios and the ratios of the $\text{H}_2\text{O}_2/\text{Ph}_2\text{S}$ conversions in these reactions are presented in Supplementary materials.

Hydroxyl radicals generation was examined by testing the reaction of terephthalic acid (TA) hydroxylation. Studied materials (0.5 g dm^{-3}) suspended in 16 cm^3 of the terephthalic acid solution (Aldrich, 98%; $3 \times 10^{-3}\text{ mol dm}^{-3}$ dissolved in 0.01 mol dm^{-3} NaOH, pH = 11) were irradiated with an XBO-150 xenon lamp (Instytut Fotonowy, 8.1 mW

cm⁻²). To avoid excitation of TA a 320 nm cut off filter was used as well as NIR and IR filter (10 cm optical path, 0.1 mol dm⁻³ solution of CuSO₄). Samples of 2 cm³ were collected during irradiation and then centrifuged to separate the photocatalyst powder. In the reaction of non-fluorescent TA with hydroxyl radicals hydroxyterephthalic acid (TAOH) is formed. Formation of TAOH was monitored by the emission spectroscopy. It shows a broad emission band at $\lambda_{\text{max}} = 425$ nm (when excited at $\lambda_{\text{exc}} = 315$ nm).

3. Results and discussion

3.1. Characterization of the samples

Chemical composition of the zeolite samples is presented in Table 1. It can be seen, that the real Si/Ti molar ratios are higher than intended values, indicating the lower titanium content in the samples than it was planned. The Si/Ti molar ratios in the analogous Ti-FER and Ti-ITQ-6 samples are slightly different. It is possible that part of titanium was removed from Ti-PREFER during its delamination. This effect is more distinct for the samples with the higher titanium content.

The X-ray diffraction patterns of the Ti-FER samples, presented in Fig. 1A, are typical of ferrierite zeolite [15]. An increase in titanium loading resulted in a decrease in intensity of the reflections, what is possibly related to decreased ordering of the zeolite framework and crystallinity of the samples with the larger Ti-content [4,16,17]. Delamination of the Ti-PREFER structure, resulting in the Ti-ITQ-6 series, decreased intensity of the reflections characteristic of ferrierite (Fig. 1B). It is related to the significantly limited long-distance ordering in delaminated structures. Similarly to the Ti-FER samples, an increase in titanium content resulted in decreased intensity of the reflections characteristic of ferrierite in the Ti-ITQ-6 series. No reflections characteristic of TiO₂ or any other titanium containing phases were identified in diffractograms of the zeolitic samples.

Nitrogen adsorption-desorption isotherms of the studied samples are presented in Fig. 2, while their textural parameters are compared in Table 2. Isotherms of the Ti-FER samples can be qualified as isotherms of the type I characteristic of microporous materials (Fig. 2A). This type of isotherm shows a steep adsorption at low relative pressure, which is assigned to nitrogen condensation in micropores [18]. Comparison of textural parameters (Table 2) of the Ti-FER samples shows only small decrease in the BET surface area from 400 m² g⁻¹ for zeolite with the lowest titanium content (Ti-FER-100) to 378 m² g⁻¹ for the sample with the highest titanium loading (Ti-FER-12.5). The changes in micropore volume (V_{MIC}) follow the same tendency. Pore size distributions, determined in the range of micropores and mesopores for a series of the Ti-FER samples, are presented in Fig. 3A. The maximum of pore size distribution in a series of the Ti-FER samples is located at about 0.53–0.57 nm, what is in full agreement with the diameter of 10 MR channels in ferrierite [19]. No peaks in the mesopore range were found in the pore size distribution profiles of the Ti-FER samples.

The nitrogen adsorption-desorption isotherms recorded for the series of the Ti-ITQ-6 samples, presented in Fig. 2B, is the type IV,

Table 1

Silicon and titanium content in the samples of Ti-FER and Ti-ITQ-6 series measured by ICP-OES method.

Sample	Si /wt%	Ti /wt%	Si/Ti /mol/mol
Ti-FER-12.5	43.6	4.0	26
Ti-FER-25	45.3	1.8	60
Ti-FER-50	46.1	0.8	137
Ti-FER-100	46.6	0.2	556
Ti-ITQ-6-12.5	44.6	2.8	38
Ti-ITQ-6-25	46.3	1.8	61
Ti-ITQ-6-50	46.3	0.5	221
Ti-ITQ-6-100	46.6	0.2	556

characteristic for mesoporous materials. Moreover, an increase in adsorbed volume of nitrogen observed at very low relative nitrogen pressure indicates also a significant contribution of micropores in this series of the samples. Micropores are located in the zeolitic layers, while mesopores are the spaces between chaotically oriented zeolite layers. The hysteresis loops are the H3 type, characteristic of non-rigid aggregates of plate like particles [20], typical of the ITQ-6 structure [21,22]. Profiles of pore size distributions in the micropore and mesopore ranges for a series of the Ti-ITQ-6 are presented in Fig. 3B. In the micropore range the maximum of pore size distribution is located at about 0.53–0.58 nm with a broad tail from the side of larger pores. Thus, the location of this maximum fits very well to the diameter of 10 MR channels in ferrierite [19]. The intensity of this maximum is significantly reduced comparing to the Ti-FER samples. In the mesopore range the maximum of pore size distribution is centered in the range of 3.7–5.1 nm. In the case of the sample with the lowest titanium content, Ti-ITQ-6-100, a sharp maximum is located at 3.7 nm with a broad tail from the side of larger pores. For other samples of this series much broader peak of mesopore size distribution was observed. Textural parameters, presented in Table 2, show significantly higher BET surface areas of the Ti-ITQ-6 samples compared to the Ti-FER series, especially in the case of zeolite with the highest titanium content (Ti-ITQ-6-12.5). Moreover, delaminated zeolites are characterized by the total pore volume of about 4–6 times larger and micropore volume significantly reduced compared to the Ti-FER samples. These results clearly show the successful delamination of Ti-PREFER resulting in Ti-ITQ-6 zeolites.

UV-vis-DRS method was used for determination the form and aggregation of titanium species introduced into zeolites. The original UV-vis-DR spectra and sub-bands obtained by their deconvolution are presented in Fig. 4. For the Ti-FER samples the intensive bands at about 220 nm, attributed to tetrahedrally coordinated Ti⁴⁺ cations incorporated into the zeolite framework, are present (Fig. 4, left side). These bands result from the ligand-to-metal charge transfer within tetrahedral TiO₄ and O₃TiOH moieties incorporated into the zeolite framework [23–25]. Moreover, the less intensive bands above 220 nm can be attributed to extraframework titanium species, such as isolated Ti⁴⁺ cations in the octahedral coordination (about 230–250 nm) and partially polymerized hexacoordinated Ti-species containing Ti–O–Ti bridges (about 260–320 nm) [5,15,26,27]. For the sample with the lowest titanium content, Ti-FER-100, the second band, at about 250 nm, is attributed to monomeric extraframework Ti⁴⁺ cations in the octahedral coordination. An increase in titanium content resulted in a gradual shift of this subband to 290, 296 and 303 nm for Ti-FER-50, Ti-FER-25 and Ti-FER-12.5, respectively. This interesting effect is related to the formation of extraframework, partially polymerized, hexacoordinated Ti-species, in which the polymerization degree increased with an increase in titanium content.

In the case of the Ti-ITQ-6 samples the original bands were deconvoluted into two subbands (Fig. 4, right side), similar to the Ti-FER samples. The first subband at about 225 nm is assigned to tetrahedrally coordinated Ti⁴⁺ cations incorporated into the zeolite framework, while the second band, at 255–285 nm, is related to a partially polymerized hexacoordinated Ti-species containing Ti–O–Ti bridges, located in the extraframework positions [5,15,26,27]. The contribution of this subband in spectra increased with an increase in titanium content. Moreover, the shift of this maximum from 255 nm for Ti-ITQ-6-100 to 285 nm for Ti-ITQ-6-12.5 indicates the tendency to the formation of polymerized titanium species in the samples with the higher titanium content.

3.2. Catalytic studies

Zeolites of the Ti-FER and Ti-ITQ-6 series were studied as catalysts for oxidation of diphenyl sulfide (Ph₂S) to diphenyl sulfoxide (Ph₂SO) and diphenyl sulfone (Ph₂SO₂) in the presence of hydrogen peroxide (H₂O₂) as an oxidant. Apart from Ph₂SO and Ph₂SO₂ no other reaction

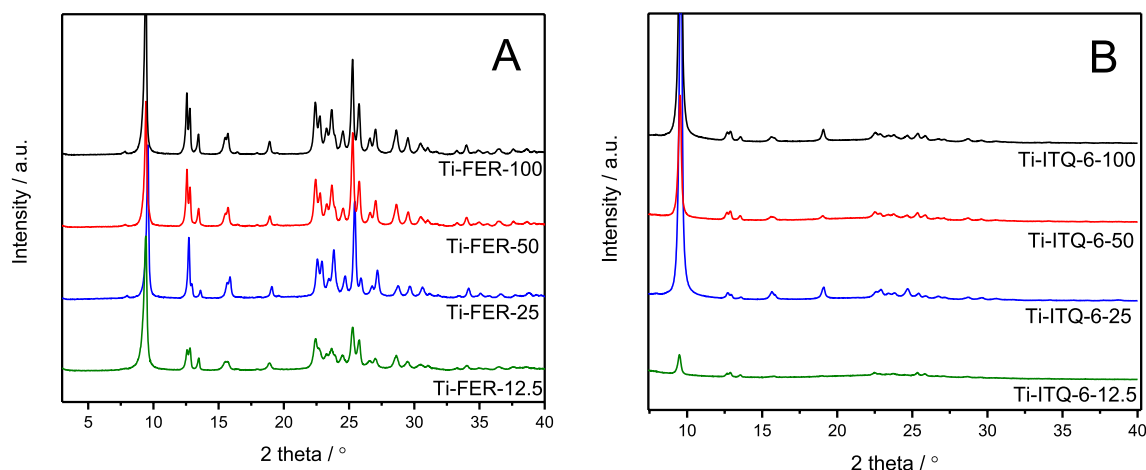


Fig. 1. X-ray diffraction patterns of Ti-substituted Ti-FER (A) and Ti-ITQ-6 (B) zeolites with different Si/Ti ratio.

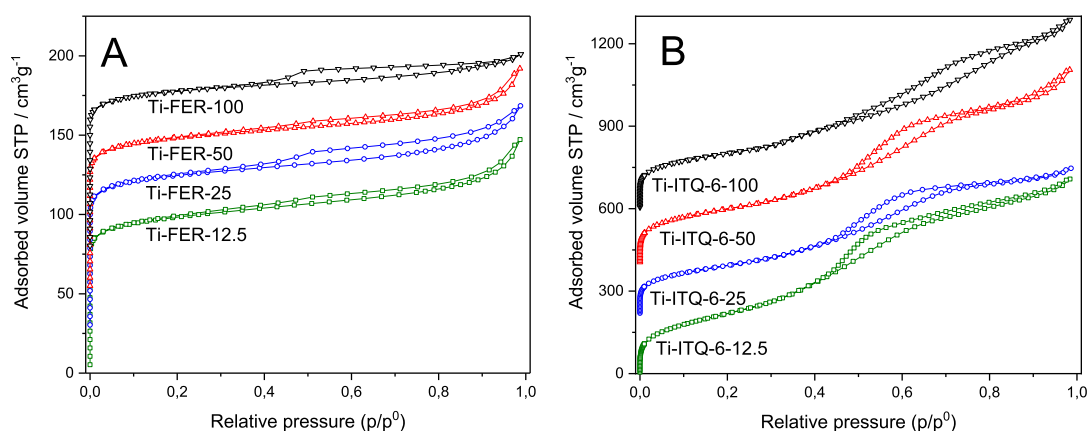


Fig. 2. N₂ adsorption-desorption isotherms of Ti-FER (intervals of 25 cm³ g⁻¹) and Ti-ITQ-6 (intervals of 200 cm³ g⁻¹) zeolites with different Si/Ti ratios.

Table 2

Textural properties of Ti-substituted FER and ITQ-6 zeolites.

Sample	S _{BET} /m ² /g	V _{MIC} /cm ³ /g	V _{TOT} /cm ³ /g
Ti-FER-12.5	378	0.136	0.228
Ti-FER-25	384	0.139	0.222
Ti-FER-50	380	0.139	0.220
Ti-FER-100	400	0.149	0.195
Ti-ITQ-6-12.5	940	0.046	1.266
Ti-ITQ-6-25	642	0.036	0.823
Ti-ITQ-6-50	721	0.056	1.092
Ti-ITQ-6-100	729	0.046	1.069

products were detected. Moreover, zeolitic samples were tested as catalysts for dimethyl sulfide (DMS) oxidation by H₂O₂. Dimethyl sulfoxide (DMSO) and dimethyl sulfone (DMSO₂) were the only detected reaction products. As it was shown in our previous paper the oxidation of Ph₂S in the absence of H₂O₂ was not effective [28].

Fig. 5 shows the results of the Ph₂S oxidation in the presence of the Ti-FER and Ti-ITQ-6 catalysts without (DARK) as well as with UV irradiation (LIGHT). As mentioned, Ph₂SO and Ph₂SO₂ were the only detected reaction products, thus the selectivity to Ph₂SO₂ can be determined by subtraction of the selectivity towards Ph₂SO from 100%. Conversion of Ph₂S depended on titanium content in the Ti-FER catalysts. In the case of the tests conducted without UV irradiation for the most effective catalyst of this series, Ti-FER-12.5, the Ph₂S conversion of about 80% was achieved after 4 h of the catalytic reaction. Other catalysts of this series were less active. The selectivities to Ph₂SO obtained

for all catalysts of this series were above 94%. The oxidation of Ph₂S in the presence of the Ti-FER catalysts was significantly improved under UV irradiation (Fig. 5). The efficiency of diphenyl sulfide oxidation, similarly to catalytic tests without UV irradiation, increased with an increase in titanium content in the Ti-FER samples. Ph₂SO was the only reaction product during the first hour of the tests and afterwards the formation of small amounts of Ph₂SO₂ was detected.

The Ti-ITQ-6 samples were found to be much more effective catalysts of Ph₂S oxidation than the catalysts of the Ti-FER series, both in the tests conducted without and with UV irradiation. Similarly to the Ti-FER series, effectiveness of Ph₂S oxidation increased with an increase of the titanium content in the Ti-ITQ-6 catalysts. In the case of the catalytic tests conducted without UV irradiation 100% of diphenyl sulfide conversion was obtained only for the sample with the highest titanium content after 2 h of the catalytic reaction. Other catalysts of this series were less catalytically active than Ti-ITQ-6-12.5, however presented significantly higher activity than the analogous catalysts of the Ti-FER series. The selectivity to Ph₂SO and Ph₂SO₂ depended on titanium content in the Ti-ITQ-6 catalysts. For the Ti-ITQ-6-12.5 catalyst, Ph₂SO₂ was the only product of Ph₂S oxidation after 3 h of the catalytic reaction. Also for other catalysts of this series the selectivity to Ph₂SO₂ was significantly higher compared to the analogous Ti-FER samples. Efficiency of Ph₂S oxidation in the presence of the Ti-ITQ-6 catalysts was significantly improved under UV irradiation (Fig. 5). In this case the complete Ph₂S conversion was obtained for the Ti-ITQ-6-25 and Ti-ITQ-6-12.5 catalysts during less than 1 h of the catalytic reaction. The other catalysts of this series were less active, however the correlation between

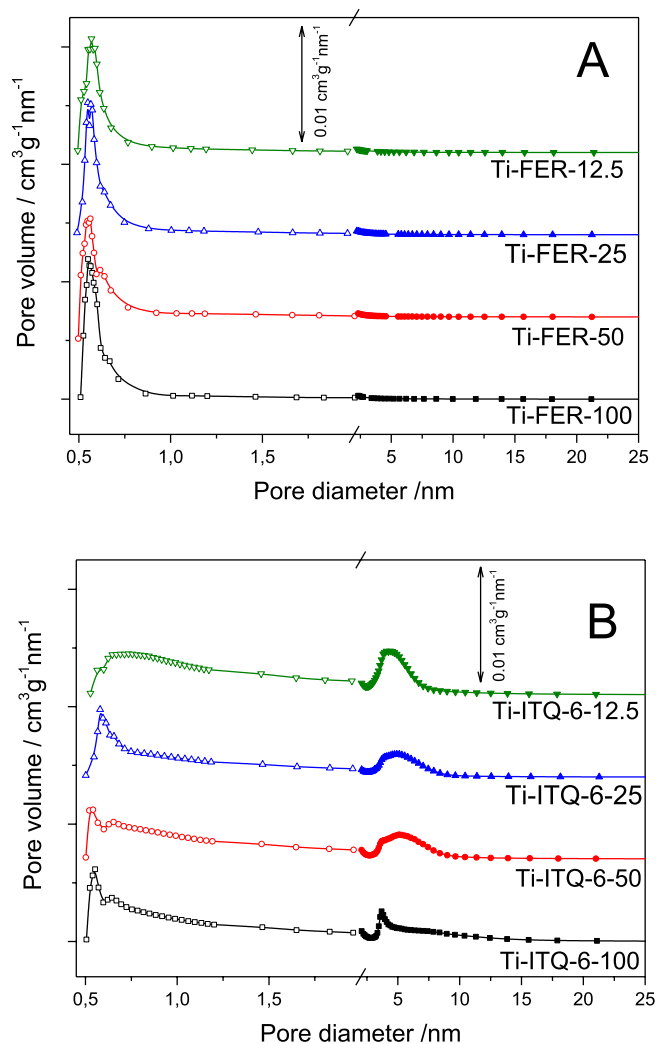


Fig. 3. Profiles of pore size distribution in micropore and mesopore ranges for Ti-FER (A) and Ti-ITQ-6 (B) zeolites with different Si/Ti ratios.

titanium content and their catalytic activity is still present. The selectivity to Ph₂SO decreased, while selectivity to Ph₂SO₂ increased during the catalytic tests. This effect is more distinct for the catalysts with the higher titanium content, however 100% selectivity to Ph₂SO₂ was obtained only for Ti-ITQ-6-12.5 after 2 h of the catalytic reaction.

Thus, efficiency of Ph₂S oxidation, taking into accounts its conversion and reaction products distribution, is much higher for the Ti-ITQ-6 catalysts than for the Ti-FER series. The correlation between Ti-content in the samples and their catalytic performance shows a very important role of titanium in this reaction. Another important issue is the porosity of the zeolitic samples. As it was shown (Fig. 3), micropores with diameter of about 0.55 nm dominate in the Ti-FER samples, while the size of diphenyl sulfide molecule, depending on its orientation and conformation, is in the approximate range of 0.24–0.93 nm. Thus, the internal diffusion of Ph₂S in micropores of Ti-FER is strongly restricted or even impossible and its oxidation possibly occurs mainly on the external surface of the zeolite crystallites. In the Ti-ITQ-6 samples, apart from micropores also interlayer mesopores are present (Fig. 3). Such mesopores with the size of 3.7–5.1 nm can easily accommodate Ph₂S molecules.

The results of the DMS oxidation in the presence of the Ti-FER and Ti-ITQ-6 catalysts are shown in Fig. 6. The oxidation of DMS, both in DARK and LIGHT conditions, is more effective than the Ph₂S oxidation for both series of the catalysts. In the case of the reaction conducted without UV irradiation the correlation between Ti-content in the samples and their

catalytic activity is not so evident. The catalysts with the lowest titanium content, Ti-FER-100 and Ti-ITQ-6-100, were significantly less effective than the other catalysts of both series. However, there are not significant differences in the DMS conversion for the catalysts with the higher titanium content. The selectivity to dimethyl sulfoxide, for both series of the catalysts is similar, about 35%. A slightly higher selectivity to DMSO was obtained in the presence of the samples with the lowest Ti-content – Ti-FER-100 and Ti-ITQ-6-100. Efficiency of DMS oxidation in the presence of both series of the catalysts was significantly improved under UV irradiation (Fig. 6). For all catalysts of both series the complete DMS conversion was obtained during 30 min of the catalytic test. In contrast to the DMS oxidation in DARK conditions, for the reaction conducted under UV irradiation there is a correlation between titanium content in the catalysts and their catalytic activity. The selectivity to DMSO decreased by about 5% under UV irradiation comparing to the reaction conducted in DARK conditions (Fig. 6).

The efficiency in DMS conversion is significantly higher comparing to Ph₂S. The size of dimethyl sulfide molecules is significantly smaller compared to diphenyl sulfide and therefore DMS molecules can penetrate not only mesopores but also micropores of the Ti-FER samples. A slightly higher efficiency of the DMS conversion, observed for Ti-ITQ-6 catalysts, is possibly related to the faster rate of the internal diffusion of reactants in the hierarchical meso- and microporous structure of this series of the samples comparing to the slower internal diffusion in micropores in Ti-FER catalysts.

Comparing the results of the catalytic oxidation of Ph₂S (Fig. 5) and DMS (Fig. 6) obtained for the Ti-ITQ-6 catalysts, it can be seen that the selectivity of diphenyl sulfide oxidation to Ph₂SO decreased, while selectivity to Ph₂SO₂ increased with the reaction time. On the other hand, the selectivities to DMSO and DMSO₂ were nearly the same during the catalytic tests. This interesting effect could be explained by different reaction mechanisms of Ph₂S and DMS oxidation. It seems that the diphenyl sulfide conversion in the presence of the Ti-ITQ-6 catalysts is a sequence of two consecutive oxidation steps: Ph₂S → Ph₂SO → Ph₂SO₂, while oxidation of DMS occurs in parallel directly to DMSO and DMSO₂.

Turnover frequency (TOF) values determined for the reactions of Ph₂S and DMS oxidation, conducted with and without UV irradiation, are compared in Table 3. It was assumed that all titanium cations play a role of catalytically active sites. TOF values were determined for the initial period of 30 min of the reactions. In general, TOF values increase with a decrease in titanium content in the samples (the only exception is Ti-ITQ-6-100). This effect could be related to the higher reactivity of Ti⁴⁺ cations incorporated into the zeolite framework comparing to the extraframework titanium species. Moreover, it was assumed that all titanium cations are accessible for the reacting molecules but in the case of extraframework, more aggregated species this may not be met. In general, TOF values determined for the conversion of DMS are higher than for the Ph₂S conversion, what is possibly related to different internal diffusion rates of smaller DME and larger Ph₂S molecules. This same trend is observed for the conversion of large Ph₂S molecules in the presence of microporous Ti-FER zeolites (lower TOF values) and micromesoporous Ti-ITQ-6 samples (higher TOF values). Moreover, in the case of the reactions conducted under UV irradiation a significant increase in TOF values was observed.

As it was shown, the organic sulfides oxidation with H₂O₂ is possible without UV irradiation, however it is significantly less effective comparing to the process conducted under UV irradiation. The catalytic oxidation of various organic compounds over zeolites containing titanium has been reported in literature [29–33]. Ravinder et al. [29] postulated the formation of Ti-hydroperoxide complexes (≡Ti–O–O–H) as a result of H₂O₂ interaction with titanium cations in titanium silicate molecular sieves. Similar results were reported for H₂O₂ interacting with Ti⁴⁺ cations, present in the Ti-silicate framework, by Bordiga et al. [30] and Tozola et al. [31]. On the other hand, the formation of such reactive Ti-hydroperoxide complexes was reported not only for monomeric Ti⁴⁺ cations in the zeolite framework but also for ≡Ti–O–Ti≡ pairs in

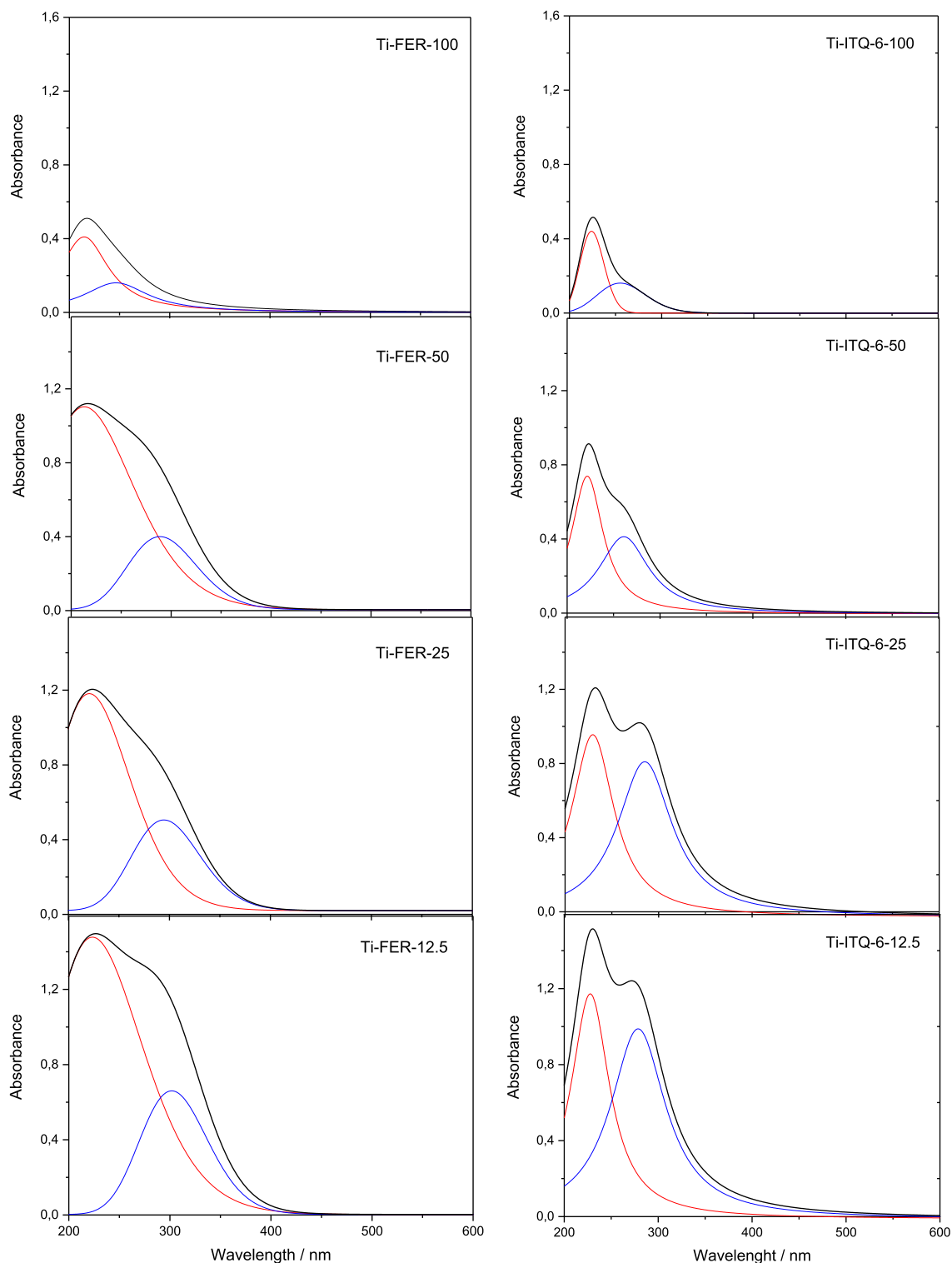


Fig. 4. UV-vis DR spectra of the Ti-FER (left) and Ti-ITQ-6 (right) zeolites with different Si/Ti ratios.

TiAlPO-5 by Novara et al. [32]. Thus, possibly also small aggregates of TiO_2 , present in the extraframework positions of zeolites, can participate in the catalytic oxidation of organic molecules. Chen et al. [33] showed that the white TS-1 powder became light yellow when TS-1 was immersed in aqueous solution of H_2O_2 , indicating the formation of titanium-hydroperoxide complexes by the direct interaction of TS-1 with H_2O_2 . A similar effect was also observed in this work for the samples of Ti-FER and Ti-ITQ-6 series, thus the formation of titanium-hydroperoxide complexes is postulated also for these catalysts.

Theoretical studies of the TS-1 catalyzed epoxidation of ethylene with H_2O_2 resulted in a conclusion that the O-O bond length in titanium-hydroperoxide complexes ($\equiv\text{Ti}-\text{O}-\text{O}-\text{H}$) is 1.521 Å, which represents a remarkable activation of the O-O bond compared to H_2O_2 molecule [34]. A high oxidation reactivity of titanium-hydroperoxide complexes was proven for sulfoxidation of thioethers [29], epoxidation of ethylene [34], oxidation of dibenzothiophene [35] and other organic compounds. Thus, oxidation of organic sulfides by H_2O_2 over the Ti-FER and Ti-ITQ-6 catalysts possibly includes the formation of

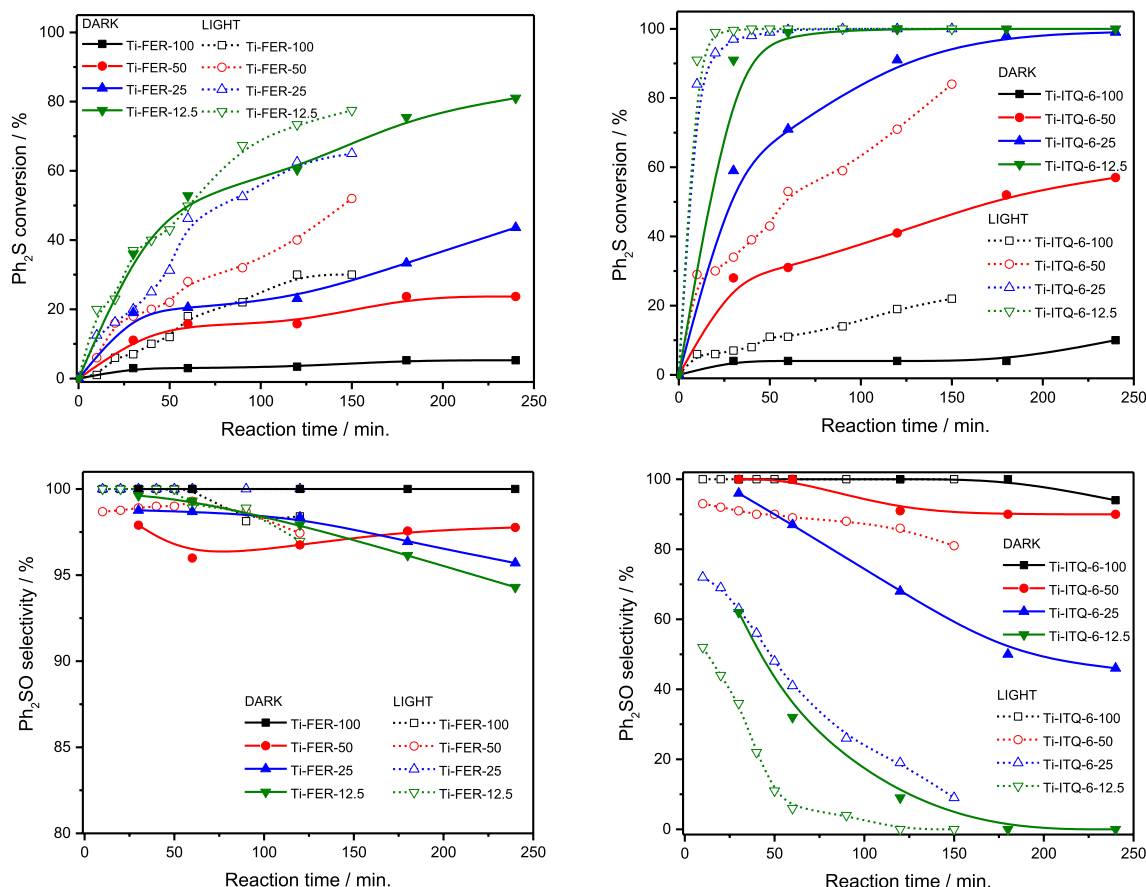


Fig. 5. The results of catalytic oxidation of Ph_2S by H_2O_2 conducted with (LIGHT) and without UV irradiation (DARK) in the presence of Ti-FER (left) and Ti-ITQ-6 (right) zeolites.

highly reactive titanium-hydroperoxide complexes ($\equiv\text{Ti}-\text{O}-\text{O}-\text{H}$), which effectively oxidize organic sulfides to sulfoxide and sulfones.

A comparison of the results of the catalytic tests conducted with and without UV radiation (Figs. 5 and 6) shows a significant intensification of organic sulfides oxidation by UV irradiation. Juan et al. [35] postulated two possible pathways of thioether oxidation by H_2O_2 over TS-1 catalysts under UV radiation. The first mechanism involves the formation of titanium-hydroperoxide complexes ($\equiv\text{Ti}-\text{O}-\text{O}-\text{H}$), which under UV radiation decompose to hydroxyl radicals (HO^\bullet), reactive in the oxidation of organic sulfides. Karlsen and Schöffel [34] as well as Dae Lee et al. [36] postulated that HO^\bullet radical can be formed much easier from titanium-hydroperoxide complexes than from H_2O_2 . The second mechanism is related to the presence of small oligomeric Ti-O-Ti-O-Ti species [35,37]. Such small aggregated species were identified in the Ti-FER and Ti-ITQ-6 samples by UV-vis-DRS analysis (Fig. 4). Howe and Krisnandi [37] reported that electron transfer may occur between the Ti-O-Ti-O-Ti chains and guest species in the pores of Ti-containing zeolite, resulting in Ti^{3+} cations in such oligomeric species. It was reported that such species play a role of a single-site photocatalyst active in the formation of free radicals involved in polymerization of ethylene [37]. A similar activity in the formation of HO^\bullet radicals from the reduction of H_2O_2 (resulting in HO^\bullet and OH^-) cannot be excluded. In order to verify the possible formation of hydroxyl radicals under UV irradiation, tests of terephthalic acid (TA) to hydroxyterephthalic acid (TAOH) oxidation by HO^\bullet radicals were done in the presence of the most active catalysts of the Ti-ITQ-6 series. The reaction rate is a measure of the efficiency of hydroxyl radicals generation in the reaction mixture. Results of these studies, presented in Fig. 7, clearly show that HO^\bullet radicals are intensively formed only under UV irradiation. Therefore, enhanced oxidation of organic sulfides in LIGHT conditions as a result of

the hydroxyl radicals formation, according to one or both described mechanisms, is postulated. Moreover, HO^\bullet radicals are well known as highly reactive, often regarded as the most effective, oxidants involved in photocatalytic processes. Because of the involvement of non-selective HO^\bullet radicals, a decreased selectivity of sulfoxides formation under irradiation was observed.

4. Conclusions

Titanosilicate ferrierite (Ti-FER) and its delaminated form (Ti-ITQ-6), with the various Si/Ti molar ratios, were synthesized and tested as catalysts for diphenyl sulfide (Ph_2S) and dimethyl sulfide (DMS) oxidation with H_2O_2 without and with UV irradiation. The main conclusions of these studies are:

1. Activity of the zeolitic catalysts in oxidation of Ph_2S and DMS, both without and with UV irradiation, increased with an increase in titanium content;
2. Conversion of Ph_2S was more effective in the presence of delaminated Ti-ITQ-6 catalysts than microporous Ti-FER. It is related to the possible internal diffusion of bulky Ph_2S molecules and products of its oxidation in mesopores of Ti-ITQ-6 catalysts. In the case of Ti-FER catalysts, due to their microporous structure, oxidation of Ph_2S possibly occurred only on the external surface of the zeolite grains;
3. Conversion of DMS was significantly more effective than Ph_2S , for both series of zeolitic catalysts, due to easy accessibility of micropores for small DMS molecule;
4. The conversion of organic sulfides was significantly intensified under UV irradiation, what was related to the UV induced decomposition of

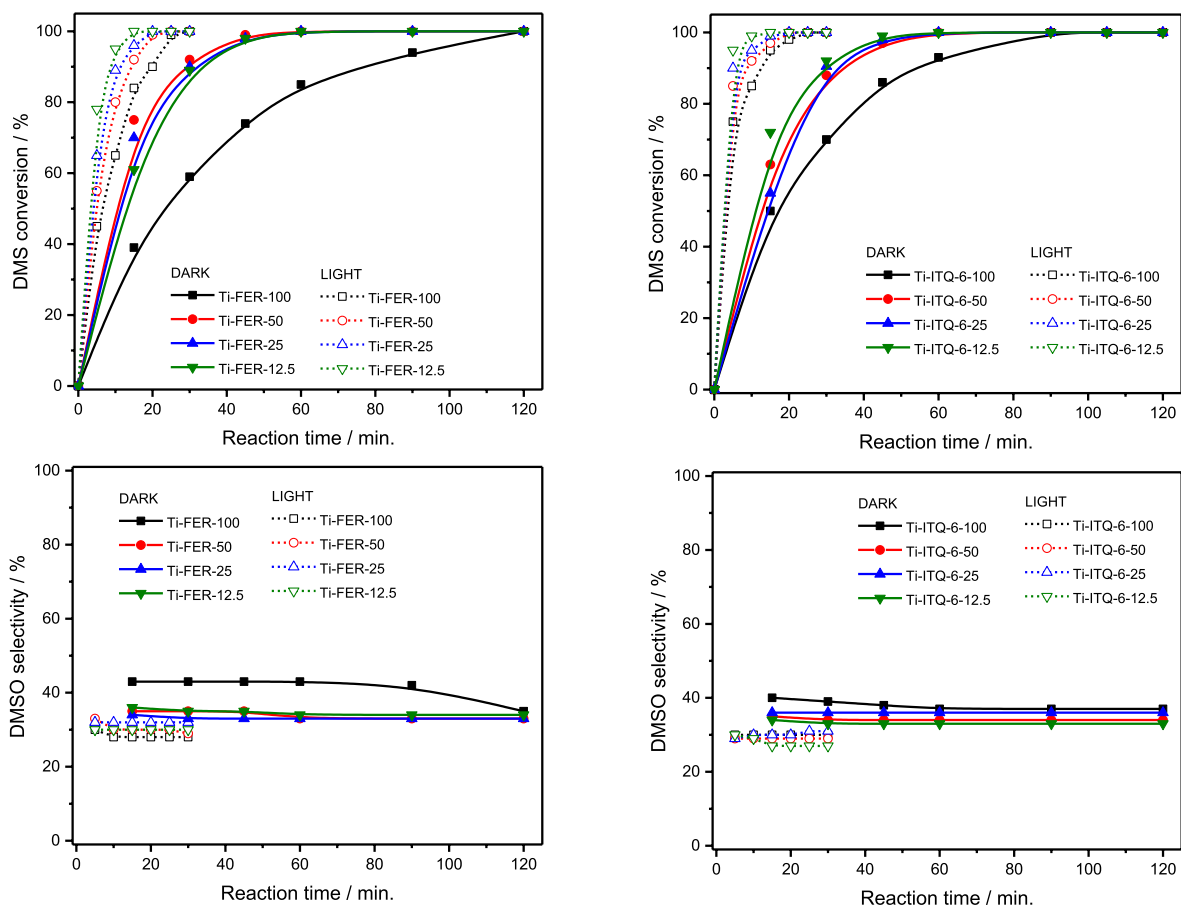


Fig. 6. The results of catalytic oxidation of DMS by H_2O_2 conducted with (LIGHT) and without UV irradiation (DARK) in the presence of Ti-FER (left) and Ti-ITQ-6 (right) zeolites.

Table 3

Turnover frequency (TOF) values determined for the initial period of the reactions (30 min).

Sample	TOF/h ⁻¹			
	Ph ₂ S (Dark)	DMS (Dark)	Ph ₂ S (Light)	DMS (Light)
Ti-FER-12.5	13.8	34.1	14.2	38.3
Ti-FER-25	16.2	76.6	17.0	85.1
Ti-FER-50	21.1	176.2	34.5	191.5
Ti-FER-100	23.0	452.0	53.6	766.1
Ti-ITQ-6-12.5	49.8	50.3	54.5	54.7
Ti-ITQ-6-25	50.2	77.0	82.6	85.1
Ti-ITQ-6-50	85.8	269.7	104.2	306.4
Ti-ITQ-6-100	30.6	536.3	61.3	766.1

H_2O_2 on titanium centers, resulting in the formation of reactive hydroxyl radicals (HO^\bullet);

- Based on the results of the catalytic studies it is postulated that conversion of Ph_2S in the presence of Ti-ITQ-6 catalysts is a sequence of two consecutive oxidation steps: $\text{Ph}_2\text{S} \rightarrow \text{Ph}_2\text{SO} \rightarrow \text{Ph}_2\text{SO}_2$, while DMS oxidation occurs in parallel directly to DMSO and DMSO_2 .

Declaration of competing interest

The authors declare that they have no known competing financial interests or personal relationships that could have appeared to influence the work reported in this paper.

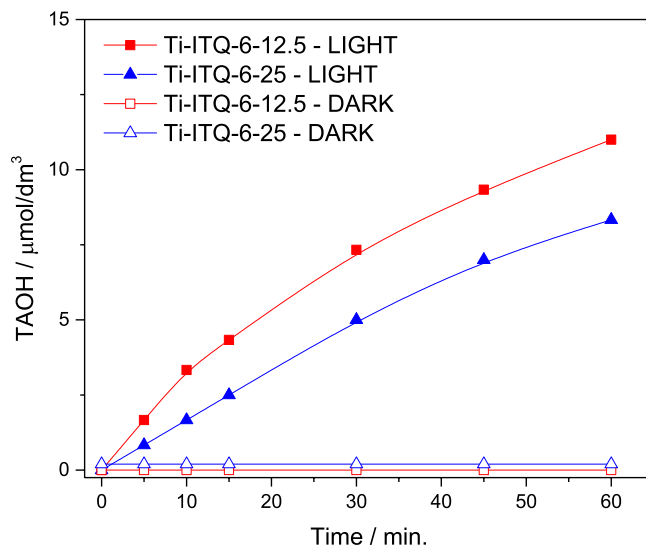


Fig. 7. Tests of terephthalic acid (TA) to hydroxyterephthalic acid (TAOH) conversion by $\bullet\text{OH}$ radicals with (LIGHT) and without (DARK) UV irradiation ($\lambda > 320 \text{ nm}$, 8.1 mW/cm^2) in the presence of the Ti-ITQ-6-12.5 and Ti-ITQ-6-25 catalysts.

CRediT authorship contribution statement

Marcelina Radko: Formal analysis. **Małgorzata Rutkowska:** Investigation, Methodology. **Andrzej Kowalczyk:** Formal analysis.

Paweł Mikrut: Formal analysis. **Aneta Świąż:** Investigation. **Urbano Díaz:** Supervision. **Antonio E. Palomares:** Methodology. **Wojciech Macyk:** Methodology, Writing - review & editing. **Lucjan Chmielarz:** Supervision, Methodology, Writing - original draft, Writing - review & editing.

Acknowledgements

The studies were carried out in the frame of project 2016/21/B/ST5/00242 from the National Science Centre (Poland). Part of the research was done with equipment purchased in the frame of European Regional Development Fund (Polish Innovation Economy Operational Program – contract no. POIG.02.01.00-12-023/08). U.D. acknowledges to the Spanish Government by the funding (MAT2017-82288-C2-1-P). The work was partially supported by the Foundation for Polish Science (FNP) within the TEAM project (POIR.04.04.00-00-3D74/16).

Appendix A. Supplementary data

Supplementary data to this article can be found online at <https://doi.org/10.1016/j.micromeso.2020.110219>.

References

- [1] J. Weitkamp, Zeolites and catalysis, *Solid State Ionics* 131 (2000) 175–188.
- [2] L. Schreyeck, P. Caullet, J.-C. Mougé, J.-L. Guth, B. Marler, A layered microporous aluminosilicate precursor of FER-type zeolite, *J. Chem. Soc., Chem. Commun.* (1995) 2187–2188.
- [3] B. Solsona, J.M. Lopez Nieto, U. Díaz, Siliceous ITQ-6: a new support for vanadia in the oxidative dehydrogenation of propane, *Microporous Mesoporous Mater.* 94 (2006) 339–347.
- [4] A. Corma, U. Díaz, M.E. Domine, V. Fornés, AlITQ-6 and TiITQ-6: synthesis, characterization, and catalytic activity, *Angew. Chem. Int. Ed.* 39 (2000) 1499–1501.
- [5] A. Corma, U. Díaz, M.E. Domine, V. Fornés, New aluminosilicate and titanosilicate delaminated materials active for acid catalysis, and oxidation reactions using H₂O₂, *J. Am. Chem. Soc.* 122 (2000) 2804–2809.
- [6] S. Shevade, R.K. Ahedi, A.N. Kotasthane, Synthesis and characterization of ferri-silicate analogs of ferrierite (Fe-FER) zeolites, *Catal. Lett.* 49 (1997) 69–75.
- [7] R. Anand, S.S. Shevade, R.K. Ahedi, S.P. Mirajkar, B.S. Rao, Epoxidation of styrene with TBHP/O₂ over ferrierite (FER) type molecular sieves, *Catal. Lett.* 62 (1997) 209–213.
- [8] A. Corma, U. Díaz, M.E. Domine, V. Fornés, Ti-ferrierite and TiITQ-6: synthesis and catalytic activity for the epoxidation of olefins with H₂O₂, *Chem. Commun.* (2000) 137–138.
- [9] I. Martausová, D. Spustová, D. Cvejn, A. Martaus, Z. Lacný, J. Přeč, Catalytic activity of advanced titanosilicate zeolites in hydrogen peroxide oxidation of methyl(phenyl)sulfide, *Catal. Today* 324 (2019) 144–153.
- [10] Y. Kon, T. Yokoi, M. Yoshioka, Y. Uesaka, H. Kujira, K. Sato, T. Tatsumi, Selective oxidation of bulky sulfides to sulfoxides over titanosilicates having an MWW structure in the presence of H₂O₂ under organic solvent-free conditions, *Tetrahedron Lett* (2013) 4918–4921.
- [11] J. Přeč, Catalytic performance of advanced titanosilicate selective oxidation catalysts – a review, *Catal. Rev.* 60 (2018) 71–131.
- [12] J. Přeč, R.E. Morris, J. Čejka, Selective oxidation of bulky organic sulphides over layered titanosilicate catalysts, *Catal. Sci. Technol.* 62 (2016) 775–2786.
- [13] K. Sato, M. Hyodo, M. Aoki, X.Q. Zheng, R. Noyori, Oxidation of sulfides to sulfoxides and sulfones with 30% hydrogen peroxide under organic solvent- and halogen-free conditions, *Tetrahedron* 57 (2001) 2469–2476.
- [14] M. Radko, A. Kowalczyk, E. Bidzińska, S. Witkowski, S. Górecka, D. Wierzbicki, K. Pamin, L. Chmielarz, Titanium dioxide doped with vanadium as effective catalyst for selective oxidation of diphenyl sulfide to diphenyl sulfonate, *J. Therm. Anal. Calorim.* 132 (2018) 1471–1480.
- [15] Q.H. Xia, T. Tatsumi, Crystallization kinetics of nanosized Tiβ zeolites with high oxidation activity by a dry-gel conversion technique, *Mater. Chem. Phys.* 89 (2005) 89–98.
- [16] A. Corma, V. Fornés, U. Díaz, ITQ-18 a new delaminated stable zeolite, *Chem. Commun.* 6 (2001) 2642–2643.
- [17] A. Chica, U. Díaz, V. Fornés, A. Corma, Changing the hydroisomerization to hydrocracking ratio of long chain alkanes by varying the level of delamination in zeolitic (ITQ-6) materials, *Catal. Today* 147 (2009) 179–185.
- [18] Z. Ramli, N. Aishikin, M. Yusoff, H. Hamdan, Delaminated zeolite, ITQ-6 as heterogeneous catalyst for Friedel Crafts alkylation, *MJAS* 11 (2007) 84–92.
- [19] H. Hu, M. Ke, K. Zhang, Q. Liu, P. Yu, Y. Liu, C. Li, W. Liu, Designing ferrierite-based catalysts with improved properties for skeletal isomerization of n-butene to isobutene, *RSC Adv.* 7 (2017) 31535–31543.
- [20] M. Thommes, K. Kaneko, A.V. Neimark, J.P. Olivier, F. Rodriguez-Reinoso, J. Rouquerol, K.S.W. Sing, Physisorption of gases, with special reference to the evaluation of surface area and pore size distribution (IUPAC Technical Report), *Pure Appl. Chem.* 87 (2015) 1051–1069.
- [21] A. Corma, V. Fornés, F. Rey, Delaminated zeolites: an efficient support for enzymes, *Adv. Mater.* 14 (2002) 71–74.
- [22] A. Zukal, I. Dominguez, J. Mayerová, J. Čejka, Functionalization of delaminated zeolite ITQ-6 for the adsorption of carbon dioxide, *Langmuir* 25 (2009) 10314–10321.
- [23] Y. Segura, L. Chmielarz, P. Kuśrowski, P. Cool, R. Dziembaj, E.F. Vansant, Characterization and reactivity of vanadia-titania supported SBA-15 in the SCR of NO with ammonia, *Appl. Catal., B* 61 (2005) 69–78.
- [24] A. Corma, From microporous to mesoporous molecular sieve materials and their use in catalysis, *Chem. Rev.* 97 (1997) 2373–2420.
- [25] T. Blanco, A. Corma, M.T. Navarro, J. Pérez-Parianta, Synthesis, characterization and catalytic activity of Ti-MCM-41 structures, *J. Catal.* 156 (1995) 65–75.
- [26] B.T. Yang, P. Wu, Post-synthesis and catalytic performance of FER type sub-zeolite Ti-ECNU-8, *Chin. Chem. Lett.* 25 (2014) 1511–1514.
- [27] L. Chmielarz, Z. Piwowarska, P. Kuśrowski, B. Gil, A. Adamski, B. Dudek, M. Michalik, Porous clay heterostructures (PCHs) intercalated with silica-titania pillars and modified with transition metals as catalysts for the DeNOx proces, *Appl. Catal., B* 91 (2009) 449–459.
- [28] M. Radko, A. Kowalczyk, P. Mikrut, S. Witkowski, W. Mozgawa, W. Macyk, L. Chmielarz, Catalytic and photocatalytic oxidation of diphenyl sulphide to diphenyl sulfoxide over titanium dioxide doped with vanadium, zinc, and tin, *RSC Adv.* 10 (2020) 4023–4031.
- [29] S. Ravinder, J. Reddy, S. Reddy, R. Kumar, P. Kumar, Sulfoxidation of thioethers using titanium silicate molecular sieve catalysts, *J. Chem. Soc. Chem. Commun.* (1992) 84–85.
- [30] S. Bordiga, F. Bonino, A. Damin, C. Lamberti, Reactivity of Ti(IV) species hosted in TS-1 towards H₂O₂-H₂O solutions investigated by ab initio cluster and periodic approaches combined with experimental XANES and EXAFS data: a review and new highlights, *Phys. Chem. Chem. Phys.* 9 (2007) 4854–4878.
- [31] G. Tozzola, M.A. Mantegazza, G. Ranghino, G. Petrini, S. Bordiga, G. Ricchiardi, C. Lamberti, R. Zullian, A. Zecchina, On the structure of the active site of Ti-silicalite in reactions with hydrogen peroxide: a vibrational and computational study, *J. Catal.* 179 (1998) 64–71.
- [32] C. Novara, A. Alfayate, G. Berlier, S. Maurelli, M. Chiesa, The interaction of H₂O₂ with TiAlPO-5 molecular sieves. Probing the catalytic potential of framework substituted Ti ions, *Phys. Chem. Chem. Phys.* 15 (2013) 11099–11105.
- [33] L.Y. Chen, S. Jaenicke, G.K. Chuah, H.G. Ang, UV absorption study of solid catalysts: interaction of framework titanium with hydrogen peroxide, *J. Electron. Spectrosc. Relat. Phenom.* 82 (1996) 203–208.
- [34] E. Karlsen, K. Schöffel, Titanium-silicalite catalyzed epoxidation of ethylene with hydrogen peroxide. A theoretical study, *Catal. Today* 32 (1996) 107–114.
- [35] Z. Juan, Z. Dishuna, Y. Liyan, L. Yongbo, Photocatalytic oxidation dibenzothiophene using TS-1, *Chem. Engineer. J.* 156 (2010) 528–531.
- [36] G.D. Lee, S.K. Jung, Y.J. Jeong, J.H. Park, K.T. Lim, B.H. Ahn, S.S. Hong, Photocatalytic decomposition of 4-nitrophenol over titanium silicalite (TS-1) catalysts, *Appl. Catal. Gen.* 239 (2003) 197–208.
- [37] R.F. Howe, Y.K. Krisnandi, Photoreactivity of ETS-10, *Chem. Commun.* (2001) 1588–1589.